# FLUID INTERFACES IN PHASE TRANSITION PROBLEMS: LATTICE-BOLTZMANN METHOD

**Fabiano G. Wolf**
fgwolf@lmpt.ufsc.br

**Luis O. E. dos Santos**
emerich@lmpt.ufsc.br

**Paulo C. Philippi**
philippi@lmpt.ufsc.br

Universidade Federal de Santa Catarina
Laboratório de Meios Porosos e Propriedades Termofísicas
Campus Universitário - Trindade
Florianópolis/SC - Brasil - 88040-900

***Abstract.*** *The Lattice-Boltzmann method has been seen as an alternative model for the computational simulation of fluid dynamics. It is based on the Boltzmann transport equation, which serves as the foundation of kinetic theory of gases. Considering its suitability for complex geometry problems, it has been widely applied for the description of fluid flow with one or more components inside porous media, especially for interfacial phenomena studies. In this work, an interaction potential among particles was used for the modelling of the liquid-vapor interface. This method makes possible the simulation of phase equilibrium through an equation of state similar to the van der Waals equation. The method allows the inclusion of interaction terms among different particles, so that liquid-solid and vapor-solid interfaces can be simulated. In this work, some simulation results are presented related to the following problems: liquid-vapor phase transition, coexistence of a liquid droplet with its vapor and liquid-vapor interactons with solid surfaces. Preliminary results show that a large diversity of physical phenomena with respect to fluid-fluid and fluid-solid interfaces can be simulated. The inclusion of thermal effects leading to the correct understanding of the role of temperature gradients in phase transition and wetting processes is still necessary.*

***Keywords:*** *Lattice-Boltzmann method, Phase transition, Liquid-vapor and fluid-solid interfaces, Wettability.*

## 1. Introduction

Presently, the study of capillary phenomena in porous media is a subject of great scientific and economic interest. This is a consequence of the constant development of computational methods and of the growing capacity of computers processing. Thus, simulation methods directly based on molecular dynamics become viable for studying complex problems in interfacial physics [Koplik et al., 1988, Thompson and Robbins, 1989, Maruyama et al., 2002]. However, these methods are still restricted to very small spatial and time scales, far away from those found in practical applications. In an attempt to take into consideration the essential aspects of the relevant micro-physics and to avoid the huge quantity of information in methods based on molecular dynamics, mesoscopic models of simplified systems of particles have been developed.

The Lattice-Boltzmann method (LBM) [Qian et al., 1992, Chen et al., 1992, Wolf-Gladrow, 2000] is based on the discretization of the Boltzmann's mesoscopic equation with the BGK [Bhatnagar et al., 1954] approach for the collision operator. In LBM, the particles distribution are restricted to a discrete lattice, where each site possesses a finite number of discrete velocities pointing to the neighbor sites. In spite of these simplifications, this discrete model recovers the Navier-Stokes equations appropriately for fluids dynamics in incompressible regime. This fact is an evidence that the macroscopic behavior of fluids does not depend on the complex microscopic dynamics involved in such systems [Wolfram, 1986].

In this work, Shan and Chen model [Shan and Chen, 1993, Shan and Chen, 1994] is used for modelling the liquid-vapor interface by including an interaction potential among the particles. This model makes possible the simulation of coexistence of liquid-vapor equilibrium through an equation of state similar to the van der Waals equation.

## 2. Lattice-Boltzmann method

The Lattice-Boltzmann method (LBM) [Qian et al., 1992, Chen et al., 1992, Wolf-Gladrow, 2000] is a mesoscopic method for the description of mechanical systems of particles. Although, it has been, historically, originated from Cellular Automata models [Frisch et al., 1986, Wolfram, 1986], recently, it has been shown [He and Luo, 1997] that LBM can be considered as based on a special discrete form of the continuous Boltzmann's equation. The LBM are build on the

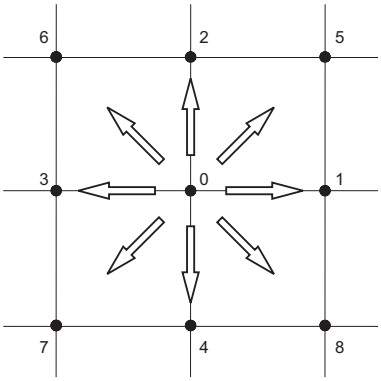


Figure 1. D2Q9 (two dimensions e nine velocities) Lattice. Note that the particles can have nine velocities, with the following magnitudes: $|\mathbf{c_0}| = 0$, $|\mathbf{c_{1,2,3,4}}| = 1$ e $|\mathbf{c_{5,6,7,8}}| = \sqrt{2}$.

mesoscopic scale, in which the system description is done using a single particle distribution function, $f_i(\mathbf{x}, t)$, representing the number of particles with velocity $\mathbf{c_i}$ at the site $\mathbf{x}$ and time t, where $i = 0 \ldots b$. In LBM, the particles are restricted to a discrete lattice, in a manner that each group of particles can move only in a finite number $b$ of directions and with a limited number of velocities (see Figure 1). Therefore, physical and velocity space are discretized. The local macroscopic properties such as total mass (the particle mass, $m$, is assumed unitary), $\rho(\mathbf{x})$, and total momentum, $\rho(\mathbf{x})\mathbf{u}(\mathbf{x})$, can be obtained from the distribution function in the following way:

$$\rho(\mathbf{x}) = \sum_i f_i \tag{1}$$

$$\rho(\mathbf{x})\mathbf{u}(\mathbf{x}) = \sum_i f_i \mathbf{c}_i. \tag{2}$$

As a result of collisions, the single particle distribution function $f_i(\mathbf{x}, t)$ is modified on each site during the time space $\Delta t$. The evolution equation that describe this change is given by

$$f_i(\mathbf{x} + \mathbf{c}_i\Delta t, t + \Delta t) - f_i(\mathbf{x}, t) = \Omega_i \tag{3}$$

where $\Omega_i$ is the collision operator. This term must be chosen in a such way to preserve total mass and momentum (and energy in isothermal problems).

The simplest form to consider the collision effects among particles is to use the collision operator introduced by Bhatnagar, Gross e Krook (BGK) [Bhatnagar et al., 1954]. It describes collision as a relaxation process to the local equilibrium state,

$$\Omega_i = -\frac{\Delta t}{\tau}(f_i - f_i^{(eq)}) \tag{4}$$

where $\tau$ is a relaxation time and $f_i^{(eq)}$ is the single particle local equilibrium distribution. Hence, the governing mesoscopic equation for the LBM will be

$$f_i(\mathbf{x} + \mathbf{c}_i\Delta t, t + \Delta t) - f_i(\mathbf{x}, t) = -\frac{\Delta t}{\tau}(f_i - f_i^{(eq)}) \tag{5}$$

After the collision step, the evolution Eq. (5) demands the local information at $\mathbf{x}$ and t, $f_i(\mathbf{x}, t)$, to be transmitted to the neighbor site $\mathbf{x} + \mathbf{c}_i\Delta t$ at time $t + \Delta t$ in the propagation step.

The macroscopic behavior of Eq. (5) can be determined by the suitable choice of the equilibrium distribution, $f_i^{(eq)} = f_i^{(eq)}(\rho, \mathbf{u})$. In the present case, one needs to recover the macroscopic dynamics of fluids ruled by Navier-Stokes equations. For this purpose, the equilibrium distribution is chosen as [Qian et al., 1992]

$$f_i^{(eq)} = g_n\rho\left[1 + \frac{c_{i\alpha}u_\alpha}{c_s^2} + \frac{u_\alpha u_\beta}{2c_s^2}\left(\frac{c_{i\alpha}c_{i\beta}}{c_s^2} - \delta_{\alpha\beta}\right)\right], \tag{6}$$

where repeated index mean summation, the $g_n$ are weight factors chosen to guarantee isotropy and $c_s$ is the sound speed on the lattice. In table 1 some examples of discrete lattices are shown .

| Lattice | $c_s$ | $g_0$ | $g_1$ | $g_2$ |
|---|---|---|---|---|
| D2Q9 | $1/\sqrt{3}$ | $4/9$ | $1/9$ | $1/36$ |
| D3Q19 | $1/\sqrt{3}$ | $1/3$ | $1/18$ | $1/36$ |

Table 1. Parameters for the lattices D2Q9 e D3Q19. The weight factors $g_0$, $g_1$ and $g_2$ correspond to that velocities with $|\mathbf{c}_0| = 0$, $|\mathbf{c}_i| = 1$ e $|c_i| = \sqrt{2}$, respectively.

Using a multiscale method such as Chapman-Enskog [Chapman and Cowling, 1970] it is possible to show that the system described above recovers the following governing equations in the incompressible regime:

$$\nabla \cdot \mathbf{u} = 0, \tag{7}$$

$$\frac{\partial \mathbf{u}}{\partial t} + \mathbf{u} \cdot \nabla \mathbf{u} = -\frac{\nabla P}{\rho} + \nu \nabla^{\mathbf{2}} \mathbf{u}, \tag{8}$$

where $P = c_s^2 \rho$ and $\nu = c_s^2(\tau - 1/2)$ are the thermodynamic pressure and the kinematic viscosity, respectively. The above equations represent the Navier-Stokes equations, for the mass and momentum conservation. The sound speed, $c_s$, can be rewritten in terms of the fraction of rest particles, $d_0$, $c = |\mathbf{c}_i|$ and from the space dimension, $D$, resulting in $c_s = \sqrt{c^2(1 - d_0)/D}$.

Next to solid surfaces, a bounce-back boundary condition [Wolf-Gladrow, 2000] is imposed for the particles leaving the fluid domain. Bounce-back condition is simply the reversion of particles momentum, assuring fluid adherence at the solid surface.

### 2.1 Inclusion of interaction potential among the particles

In order to take into account the physical ingredients found in the microscopic interactions among molecules (or atoms) of a fluid, Shan e Chen [Shan and Chen, 1993] introduced an interaction potential among particles in the LBM. In this way, the model is able to reproduce the liquid-vapor phase transition and the coexistence of two distinct phases of a single component in equilibrium, the density distribution allowing automatically to identify both phases. The authors used the following interaction potential energy between a pair of particles group localized at the sites **x** and **y**:

$$V(\mathbf{x}, \mathbf{y}) = \varphi(\mathbf{x}) G_i(\mathbf{x}, \mathbf{y}) \varphi(\mathbf{y}), \tag{9}$$

where, considering the lattices in Table 1, $G_i(\mathbf{x}, \mathbf{y}) = \mathcal{G}$ for $|\mathbf{y} - \mathbf{x}| = \sqrt{2}$, $G_i(\mathbf{x}, \mathbf{y}) = 2\mathcal{G}$ for $|\mathbf{y} - \mathbf{x}| = 1$ and $G_i(\mathbf{x}, \mathbf{y}) = 0$ otherwise. The function $\varphi$ is locally dependent on the density. Note that the magnitude of $\mathcal{G}$ determine the potential strength between the particles at **x** and **y,** while the sign defines if the potencial is attractive or repulsive.

The resulting force is given by

$$\mathbf{F}_\sigma(\mathbf{x}) = -\varphi(\mathbf{x}) \sum_i G_i \varphi(\mathbf{x} + \mathbf{c_i} \Delta t) \mathbf{c_i}. \tag{10}$$

A similar form of interaction potential was used by Martys and Chen [Martys and Chen, 1996], for the case of a fluid interacting with a solid. In that situation, the resulting force in site **x,** at time t is given by

$$\mathbf{F_w}(\mathbf{x}) = -\rho(\mathbf{x}) \sum_i W_i s(\mathbf{x} + \mathbf{c_i} \Delta t) \mathbf{c_i} \tag{11}$$

where, considering the lattices in Table 1, $W_i(\mathbf{x}, \mathbf{y}) = \omega$ for $|\mathbf{y} - \mathbf{x}| = \sqrt{2}$, $W_i(\mathbf{x}, \mathbf{y}) = 2\omega$ for $|\mathbf{y} - \mathbf{x}| = 1$ e $W_i(\mathbf{x}, \mathbf{y}) = 0$ otherwise. In the above expression, $s = 1$ represent that the nearest neighbor site is solid, while $s = 0$ represent that the nearest neighbor site is fluid.

Thus, the local velocity**,** $\mathbf{u}(\mathbf{x})$**,** in the equilibrium distribution (6) is modified by the interactions with the neighborhood in the following way:

$$\mathbf{u}' = \mathbf{u} + \frac{\tau}{\rho} \left( \mathbf{F}_\sigma + \mathbf{F_w} \right).$$

Again, the Chapman-Enskog method allows to determine the macroscopic behavior of this system. The only difference with respect to that governing equation obtained previously is the existence of a non-ideal equation of state (see Figure 2):

$$P = \frac{c^2}{D} \left[ (1 - d_0)\rho + \frac{\mathcal{G} b}{2} \varphi^2(\rho) \right]. \tag{12}$$

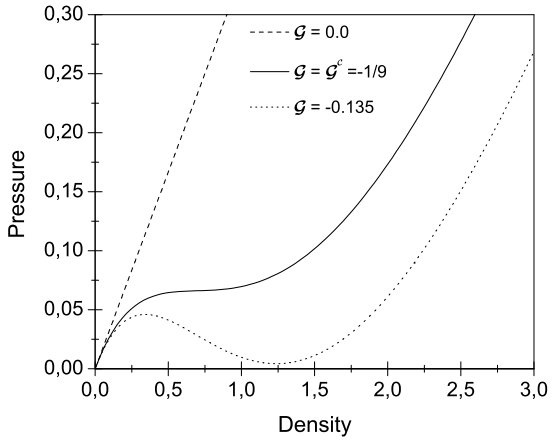


Figure 2. Pressure versus density for different values of $\mathcal{G}$. The critical value $\mathcal{G}_c$ can be obtained from $\partial P/\partial\rho = \partial^2 P/\partial\rho^2 = 0$ at the critical point.

According to Shan and Chen [Shan and Chen, 1993], for a thermodynamically consistent isothermal process, $\varphi(\rho)$ must be chosen as:

$$\varphi(\rho) = \varphi_0 exp(-\rho_0/\rho), \tag{13}$$

where $\rho_0$ e $\varphi_0$ are arbitrary constants. In the equation of state above, Eq. (13), the parameter $-(1-d_0)/\mathcal{G}$ has the same role of the temperature in the van der Waals theory. In this way, temperature can be modified by changing the fraction of particles at rest and the strength of the interaction field [Shan and Chen, 1993].

## 3. Results and discussion

To test the ability of Shan and Chen model [Shan and Chen, 1993] to simulate different kind of interaction interfaces, simulations were performed involving the liquid-vapor, the liquid-solid and vapor-solid interfaces. Unless stated otherwise, the simulations were carried out on a D2Q9 lattice with the parameters $\tau = 1$ e $\mathcal{G} = 0.15$, resulting in a density ratio of $\rho_L/\rho_V \sim 20$. Following [Shan and Chen, 1993], the function $\varphi(\rho) = 1 - exp(-\rho)$ was used, instead of Eq. (13). These functions show a similar behavior, however this choice leads to a better stability in the simulations. At the fluid boundaries of the simulation domain periodic boundary conditions were imposed.

### 3.1 Surface tension

The surface tension of liquids results of the disbalance of intermolecular forces at interfacial regions, in which exists an abrupt variation of the density. In this way, the resulting force in a molecule near the liquid-vapor interface is different from the force suffered by a molecule in a completely homogeneous region (where the resulting force is null). For a droplet in equilibrium with its vapor, the tension surface increases the internal pressure of the droplet, according to Young-Laplace law:

$$P_i - P_e = (D-1)\frac{\sigma}{R},$$

where $P_i$ , $P_e$, $\sigma$, $R$ and $D$ represent internal and external pressure, the surface tension, the droplet radius and the space dimension, respectively.

The Young-Laplace law tells that the internal pressure of the droplet can be modified by the surface tension variation and by the droplet radius. For an isothermal process, the surface tension does not suffer any variation. Then, to test the validity of the Young-Laplace law for the model described above, one can vary droplet radius and measure the corresponding pressure variation. With the graph $(P_i - P_e) \times 1/R$ it is possible to determine the surface tension directly from the angular coefficient of the straight line. The obtained results are shown in Figure 3. It is noticed $\sigma \sim 0.086$ for the surface tension, once the linearity between the pressure difference and the inverse of the radius is obtained from linear fit.

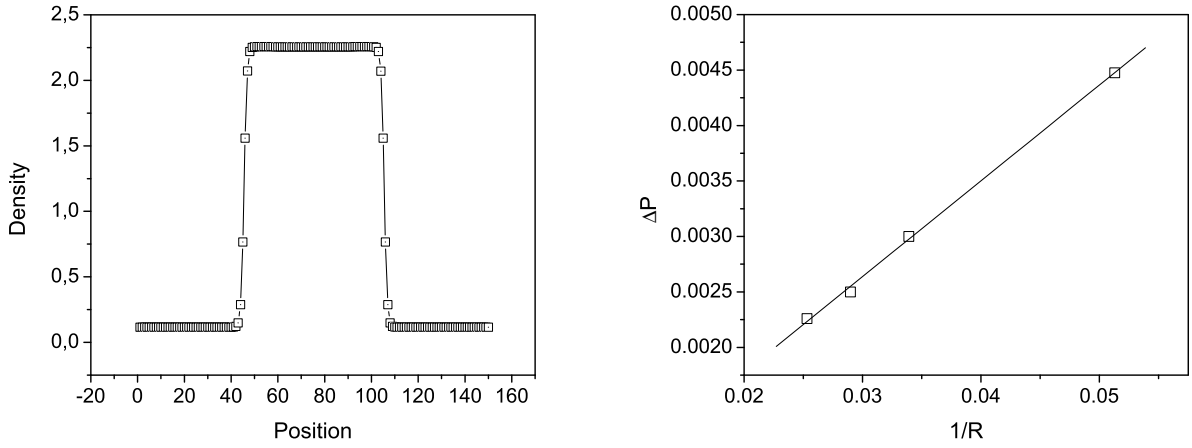


(a) (b)

Figure 3. (a) Density profile of a droplet immersed in its own vapor on a lattice size of $150 \times 150$ sites. (b) Verification of Young-Laplace law for the model described in the text.

### 3.2 Phase transition

Phase transition refers to a process in which liquid can be transformed in vapor (or vice-versa) by changing the thermodynamics variables like pressure, temperature and volume. For instance, it is possbile to transform vapor contained inside a chamber into liquid, from its volume reduction at constant temperature. In the same way, the heated vapor can be transformed in liquid by decreasing the temperature at constant volume, until a transition point, in which small liquid droplets begin to appear in the recipient.

Physically, the temperature reduction reduces the kinetic energy of molecules and the effects of collisions until a limit, where intermolecular forces become dominant, inducing the local aggregation of molecules. As mentioned previously, in Shan e Chen model, the parameter with the same role of temperature is given by $-(1-d_0)/\mathcal{G}$. Thus, temperature can be modified by the fraction of particles at rest, $d_0$, and by the intensity of interaction, given by $\mathcal{G}$. By reasons of numerical stability, $d_0$ is often assumed to be $1/3$. Hence, only the modification of $\mathcal{G}$ it will allow to simulate the temperature effect on the system.

To make the simulation of the liquid-vapor phase transition using LBM, a lattice with size of $200 \times 200$ sites was filled with a local density $\rho = \rho_0(1+z)$, where $\rho_0$ is a reference density and $z$ is a randomic perturbation being in the range $[-0.01, +0.01]$. This statistical perturbation is necessary, because it will induce the phase transition in favorable conditions. The critical value $\mathcal{G}_c$, from which the system reachs favorable conditions to the phase transition, can be obtained from the equation of state, remembering that there is an inflection point (see Figure 2):

$$\left(\frac{\partial P}{\partial \rho}\right)_{\mathcal{G}_c,\rho_c} = \left(\frac{\partial^2 P}{\partial \rho^2}\right)_{\mathcal{G}_c,\rho_c} = 0.$$

Solving the equation above, one gets

$$\mathcal{G}_c = -\frac{4(1-d_0)}{b} = -\frac{1}{9},$$

$$\rho_c \simeq 0.693.$$

In the determination of critical values above, it was considered that a D2Q9 lattice is a projection on the two-dimensional space of the face centered hypercube lattice (FCHC) [d'Humières and Frish, 1986], in which $D = 4$ and $b = 24$.

It is verified from the simulation results, that the phase transition is very quick in the beginning of process, but it becomes slower due to the large amount of small droplets competing for those particles which are still in the vapor phase. In Figure 4, it can be seen that droplets with smaller radius are more unstable than the greater droplets. That is due to surface tension effects on the interface with a larger curvature, which leads to an increase in the pressure difference in the smaller droplets, in a way that these tend to evaporate, while those greater droplets tend to grow. In Figure 5 it is shown the behavior of the liquid and vapor phases and the ratio between them for different values of $|\mathcal{G}|$. The theoretical prediction of the critical value $\mathcal{G}_c \sim -1/9$ seems to be confirmed by the simulations, considering the tendency observed.

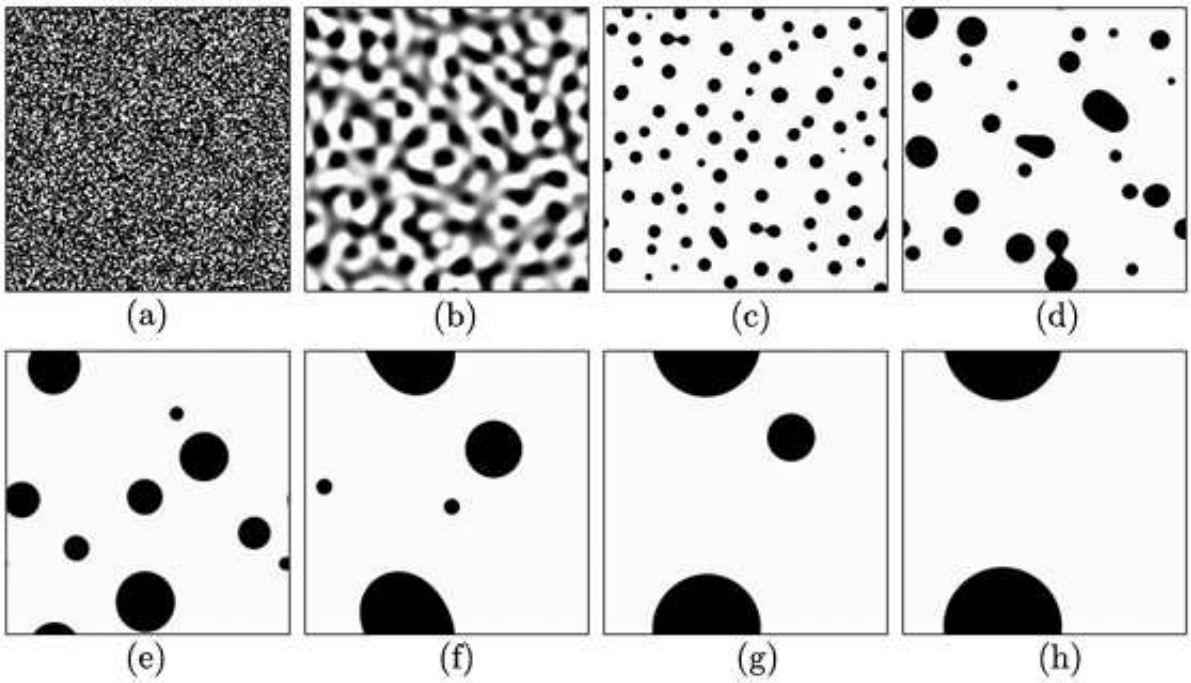


Figure 4. Phase transition simulated for $\rho_0 = 1.2$ e $\mathcal{G} = -0.15$. The evolution of the process is given from (a) to (h), in which the dark regions possess a greater density, being identified as the liquid phase.

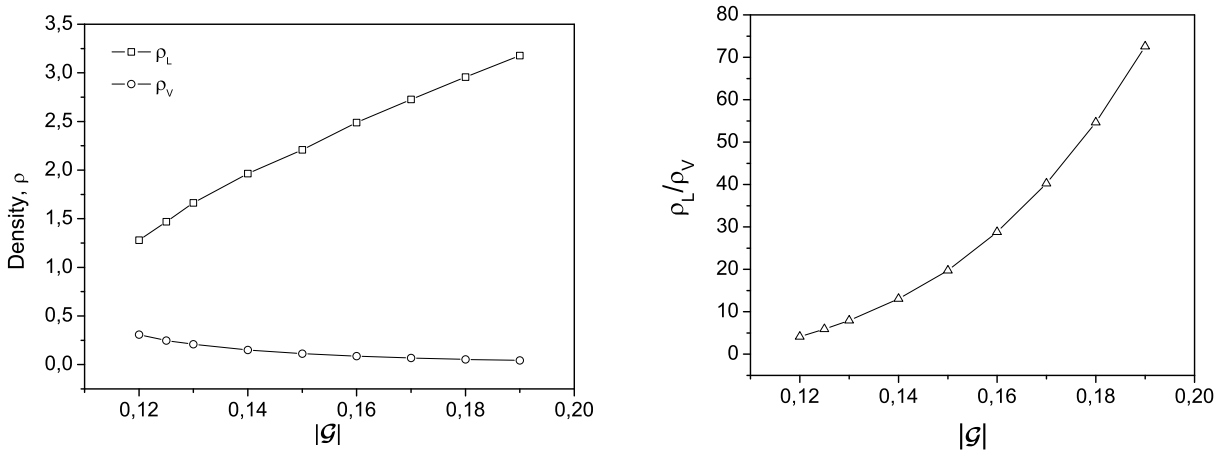


(a) (b)

Figure 5. (a) Densities of liquid and vapor phases and (b) ratio between them as a function of $|\mathcal{G}|$ from several simulations of phase transition. Note that the value of $\mathcal{G}_{max} \simeq -0.19$ is the limit value for the implemented algorithm, implying in $(\rho_L/\rho_V)_{max} \sim 72$.

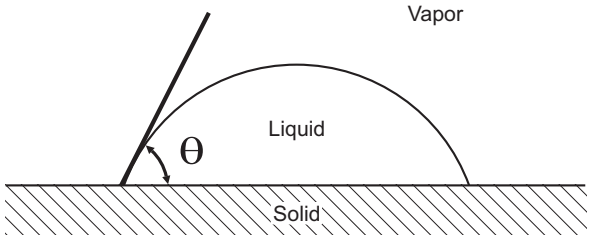


Figure 6. Illustration of the contact angle of a wetting droplet on a solid surface.

### 3.3 Wettability

Wettability is the result of molecular interactions existent between both the fluids (for instance, liquid and vapor) and the solid substrate. When liquid and vapor are in contact with a solid surface, one observes the existence of a common line among the three phases, named contact line. This configuration gives origin to the definition of the contact angle, $\theta$, as the resulting angle between the tangent line on the interface which divides liquid and vapor and that parallel line to the solid surface, as it is shown in the Figure 6. In general, if $\theta < 90°$(tipically a air-water-glass system), the liquid is *wetting* to that solid, while if $\theta > 90°$(tipically a air-mercury-glass system), the liquid is *non-wetting* to that solid.

In LBM, the relation between the cohesion forces (fluid-fluid interactions) and adhesion forces (fluid-solid interactions), which determines the contact angle, can be simulated through the introduction of the forces given by the Eq. (10) and (11). The simulation was initialized with a liquid droplet in contact with a solid. In equilibrium conditions, the contact angle was measured using the following relation (that assumes spherical approximation):

$$tan\left(\frac{\theta}{2}\right) = \frac{2H}{D}, \tag{14}$$

where *H* and *D* are the height and droplet base diameter, respectively.

The obtained results are shown in Figures 7 and 8. Wettability, given by the contact angle, is dependent on the fluid-solid potential strength, which in the present model is given by $\omega$ (Eq. 11). This dependency is shown in Figure 8. In this manner, a broad variety of capillary phenomena can be studied using this model, especially in porous media that possess a large grande spatial variability, in which the invasion capillary process can be very complicated and difficult to simulate by means of convencional methods based on the purely macroscopic approaches.

## 4. Conclusion

In this work, we show sample cases involving the application of the *Lattice-Boltzmann* method to the physical modelling of liquid-vapor, liquid-solid and vapor-solid interfaces. Despite the fact that just simple physical systems have been considered, it is evident that the method is able to simulate a large variety of complex phenomena, whose the complete understanding is not yet available. This flexibility is consequence of the fact that physical properties, like surface tension and contact angle, are resultant of mesoscopic interactions among aggregations of particles. This characteristic becomes the method applicable to the porous media with a large spatial variability, without any additional implementation difficulties and computational requirements. The inclusion of thermal effects leading to the correct understanding of the role of temperature gradients in phase transition and wetting processes is still necessary.

## 5. Acknowledgements

To the financial support by National Agency of Petroleum (ANP) and Projects and Studies Supporter (FINEP).

## 6. References

Bhatnagar, P. L., Gross, E. P., and Krook, M. (1954). A model for collision processes in gases. i. small amplitude processes in charged and neutral one-component systems. *Phys. Rev.*, 94(511).

Chapman, S. and Cowling, T. G. (1970). *The mathematical theory of non-uniform gases*. Cambridge University Press, 3rd edition.

Chen, H., Chen, S., and Matthaeus, W. H. (1992). Recovery of the Navier-Stokes equations using a lattice-gas Boltzmann method. *Physical Review A*, 45(8):R5339–5342.

d'Humières, D. Lallemand, P. and Frish, U. (1986). Lattice gas models for 3d hydrodynamics. *Europhys. Lett.*, 2:291–297.

Frisch, U., Hasslacher, B., and Pomeau, Y. (1986). Lattice-gas automata for the navier-stokes equations. *Physical Review Letters*, 56(14):1505–1508.

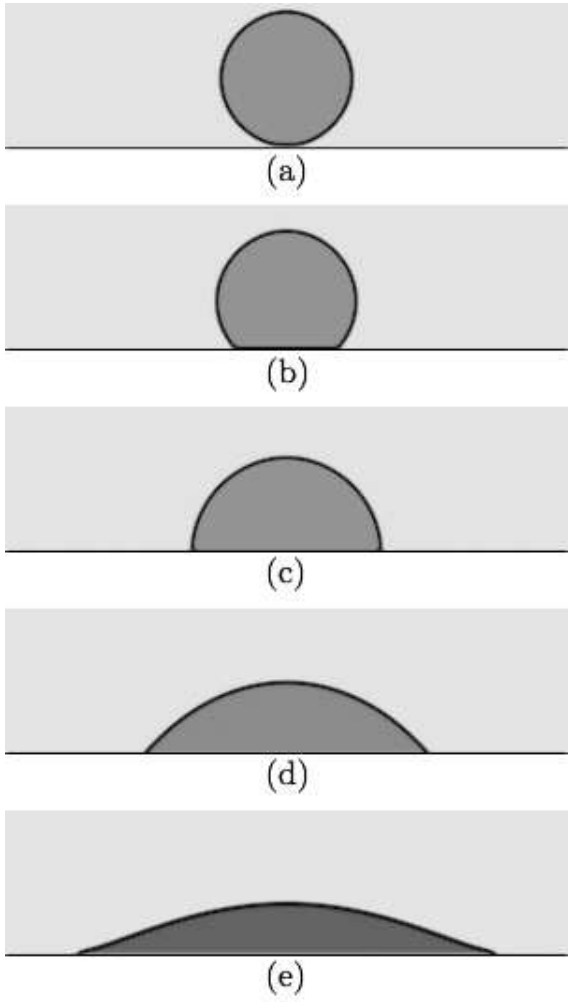


Figure 7. Equilibrium configurations of a droplet on the contact with a solid surface. From (a) until (e) the following $\omega's$ were adjusted to: 0.02, 0.035, 0.048, 0.0575 e 0.065. It is noted that the increase of adhesion forces leads to a decrease in the contact angle.

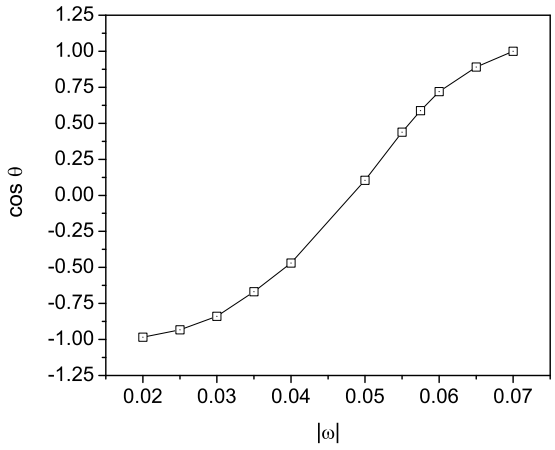


Figure 8. Cosine of the contact angle as a function of the adhesion forces.

He, X. and Luo, L. S. (1997). Theory of lattice Boltzmann method: From the Boltzmann equation to the lattice Boltzmann equation. *Physical Review E*, 56(6):6811–6817.

Koplik, J., Banavar, J. R., and Willemsen, J. F. (1988). Molecular dynamics of poiseuille flow and moving contact lines. *Physical Review Letters*, 60(13).

Martys, N. S. and Chen, H. (1996). Simulation of multicomponent fluids in complex three-dimensional geometries by the lattice Boltzmann method. *Physical Review E*, 53(1):743–750.

Maruyama, S., Kimura, T., and Lu, M. (2002). Molecular scale aspects of liquid droplet on a solid surface. *Thermal Science and Engineering*, 10(6).

Qian, Y. H., d'Humières, D., and Lallemand, P. (1992). Lattice BGK models for Navier-Stokes equations. *Europhysics Letters*, 17(6):479–484.

Shan, X. and Chen, H. (1993). Lattice Boltzmann model for simulating flows with multiple phases and components. *Physical Review E*, 47(3):1815–1819.

Shan, X. and Chen, H. (1994). Simulation of nonideal gases and liquid-gas phase transitions by the lattice Boltzmann equation. *Physical Review E*, 49(4):2941.

Thompson, P. A. and Robbins, M. O. (1989). Simulation of contact line motion: slip and the dynamic contact angle. *Physical Review Letters*, 63(7).

Wolf-Gladrow, D. (2000). *Lattice gas cellular automata and lattice Boltzmann models: An introduction*. Springer-Verlag, Berlin, 308 pp.

Wolfram, S. (1986). Cellular automaton fluids 1: Basic theory. *Journal of Statistical Physics*, 45(3/4):471–526.

## 7. Responsibility notice

The author(s) is (are) the only responsible for the printed material included in this paper